Organo Group-13 Transition-Metal Complexes, XII[◇]

Transition-Metal-Substituted Gallanes: Synthesis and Spectroscopic Studies of Highly Polar σ(M−Ga) Bonds, Structures of *trans*-$(Ph_3P)(CO)_3Co-Ga[(CH_2)_3N(C_2H_5)_2]R$ (R = Cl, CH_3) and $(\eta^5\text{-}C_5H_5)(CO)_2Fe-GaCl_2[N(CH_3)_3]$[☆]

Roland A. Fischer*, Alexander Miehr, and Thomas Priermeier

Anorganisch-chemisches Institut der Technischen Universität München, Lichtenbergstraße 4, D-85747 Garching

Received March 10, 1995

Key Words: Organogallium complexes / Cobalt−gallium bonds / Iron−gallium bonds / MOCVD / CoGa thin films

The salt elimination reaction of the transition carbonyl metallates $[L(CO)_nM](Na/K)$ (M = Cr, Mo, W, Mn, Re, Fe, Co, Ni; L = CO, $\eta^5\text{-}C_5R_5$, PR_3; n = 1−4; R = alkyl, aryl) with the base-stabilized galliumhalides $Cl_aGaR_{3-a}(Do)$ (R = H, alkyl, halide; Do = THF, $N(CH_3)_3$, NC_7H_{13}) or $Cl_aGa[(CH_2)_3NR'_2](R)_{2-a}$ yielded almost quantitatively the transition metal-substituted, gallanes $[L(CO)_nM]_aGaR_{3-a}(Do)$ and $[L(CO)_nM]_aGa[(CH_2)_3NR'_2](R)_{2-a}$, respectively. Residual halide functionalities in these complexes were selectively replaced by various other groups. The new compounds were characterized by means of elemental analysis, ^1H-, ^{13}C-, ^{31}P-NMR, MS, and IR ν(CO) data. The single-crystal X-ray structure analysis of *trans*-$(Ph_3P)(CO)_3Co-Ga[(CH_2)_3N(C_2H_5)_2](R)$ (**6s**: R = Cl, **6t**: R = CH_3) showed σ(Co−Ga) lengths of 237.78(4) and 249.5(1) pm, respectively. A short σ(Fe−Ga) contact of 236.18(3) pm was found for $(\eta^5\text{-}C_5H_5)(CO)_2Fe-GaCl_2[N(CH_3)_3]$ (**5a**). Low-pressure MOCVD experiments were performed to give thin films of analytically pure CoGa alloy.

The chemistry of transition metal-substituted gallanes is currently attracting increasing attention, because of their potential as single source precursors to deposit binary intermetallic materials, e.g. β-CoGa and η-MnGa, by low-pressure metal organic chemical vapor deposition[1]. But apart from this potential application in microelectronics, this class of compounds is also interesting from a puristic chemical point of view. Firstly, non-bridged and highly polar metal metal bonds are rather popular at the moment[2]. In this respect the σ(M−E) systems (E = Al, Ga, In; M = transition metal) are the direct main group analogs of transition metal lanthanoide and actinoide complexes, which have a long tradition[3]. Secondly, base-free R_2E moieties are isolobal to cationic carbenoid groups such as silylenes, germylenes, and stannylenes. (The C_s-symmetric $E(R')(NR_3)$ moieties may be viewed as the corresponding neutral congeners.) Thus, they are potential candidates for π-interactions with electron-rich transition metal fragments, which is probably the case for *cis*-$[Cy_2PCH_2CH_2PCy_2](R)Pt-ER_2$ (Cy = *cyclo*-C_6H_{11}; E = Ga: R = CH_2tBu; E = In: R = CH_2SiMe_3)[4,17]. To the best of our knowledge, Table 1 summarizes all compounds with (unbridged) M−Ga bonds which have been structurally characterized to date. In this paper we give a comprehensive account on our studies of the synthesis, properties and structural aspects of new M−Ga bonded compounds.

[◇] Part XI: Ref.[11].

A. Synthesis

The monovalent carbonyl metallates $[(CO)_nM](Na/K)$ (M = Mn, Re, Co; n = 5, 4), which were suspended in non-polar and non-coordinating solvents (*n*-pentane, toluene) reacted with the base-stabilized alkylgallium chlorides $ClGa(R)_2(Do)$ (R = Cl, H, Et; Do = NMe_3, $C_7H_{13}N$) quantitatively above −20 °C within minutes to yield the soluble complexes **4a**−**d**, **5a**−**b**, **6a**−**c** (Scheme 1, Table 2). The hydrido compounds **4b**, **5b**, and **6b** are difficult to handle, which is due to their extreme sensitivity to air and temp. (>0 °C). For this reason, a satisfactory elemental analysis could not be obtained for **5b**. The gallium center is coordinatively saturated by adduct formation with one molecule of a Lewis base donor. Without such a base equivalent the substitution reaction (and the alkali halide elimination) does not take place. The same was observed, if polar coordinating solvents, e.g. THF, dimethoxyethane and acetonitrile or HMPT were used. Then the solution ν(CO)-IR spectra exhibit the ν(CO) absorption bands of the unchanged carbonyl metallates. The intramolecularly adduct-stabilized organogallium chlorides $Cl_aGa[(CH_2)_3NR'_2](R_{2-a})$ (a = 1, 2; R' = Me, Et) selectively gave mono- and disubstituted compounds when treated with stoichiometric quantities of the carbonyl metallates mentioned above. No external Lewis base was necessary in these cases. In contrast to this, the *substituted* monovalent compounds $[L(CO)_nM](Na/K)$ (L = PR_3, Cp; M = Cr, Mo, W, Mn, Fe, Ru, Co, Ni; n = 1−4) reacted with gallium chlorides in po-

  0009−2940/95/0808−0831 $ 10.00+.25/0

Table 1. Structurally characterized transition-metal gallium complexes to date (Cy = *cyclo*-C_6H_{11}; Np = CH_2tBu; CN = coordination number)

Compound	CN	M-Ga [pm]	Ref.
$Cp(CO)_3W\text{-}GaMe_2$	3	270.8(3)	[5]
$[Cp(CO)_3W]_3Ga$	3	273.9(3)	[6]
$[Re_2I_2\{Ga[Re(PPh_3)(CO)_4]\}\{PPh_3\}_2(CO)_4]$	3	251.3(4)	[7]
$[Re_2Br_2\{Ga[Re(PPh_3)(CO)_4]\}\{PPh_3\}_2(CO)_4]$	3	250.3(3)	[8]
$Mn_2(CO)_8\{\mu\text{-}GaMn(CO)_5\}_2$	3	245.1(1)	[9]
$Re_2(CO)_8\{\mu\text{-}GaRe(CO)_5\}_2$	3	258.9(3)	[10]
$(CO)_5Mn\text{-}Ga(Cl)(2,4,6\text{-}{}^tBuC_6H_2)$	3	249.5(4)	[11]
$(\mu\text{-}O)[(CO)_5Mn\text{-}Ga(2,4,6\text{-}{}^tBuC_6H_2)]_2$	3	253.3(3)	[11]
cis-$[Cy_2P(CH_2)_2PCy_2](Np)Pt\text{-}GaNp_2$	3	243.8(1)	[17]
$Cp(CO)_2Fe\text{-}Ga(^tBu)_2$	3	241.7(2)	[12]
$[Cp(CO)_2Fe]_3Ga$	3	244.4(1)	[13]
$[(CO)_4Co]_2Ga(2,4,6\text{-}{}^tBuC_6H_2)$	3	249.7(2)	[11]
$[(CO)_5Mn]_2Ga[(CH_2)_3NMe_2]$	4	265.3(5)	[11]
$[Mn_3(CO)_{12}(\mu\text{-}GaCl_2)]^{2-}$	4	269.1(4)	[14]
$Cp'(CO)_3Mo\text{-}GaI_2(OEt_2)$	4	258.2(2)	[15]
$[(CO)_4Fe\text{-}Ga(\eta^1\text{-}C_2H_3)(THF)]_2$	4	251.5(2)	[16]
$Cp(CO)_2Fe\text{-}Ga(\eta^1\text{-}Cp')(NC_5H_5)$	4	242.7(1)	[16]
$Cp(CO)_2Fe\text{-}GaCl_2(NMe_3)$	4	236.1(1)	[*]
$Cp(CO)_2Fe\text{-}Ga[(CH_2)_3NMe_2](BH_4)$	4	237.5(1)	[1f]
$Cp(CO)_2Fe\text{-}Ga[(CH_2)_3NMe_2](Et)$	4	245.7(1)	[1f]
$(CO)_4Co\text{-}GaNp_2(THF)$	4	257.8(1)	[1a]
$(PPh_3)(CO)_3Co\text{-}Ga[(CH_2)_3NEt_2](CH_3)$	4	249.6(1)	[*]
$(PPh_3)(CO)_3Co\text{-}Ga[(CH_2)_3NEt_2](Cl)$	4	237.8(1)	[*]
$[(CO)_4Co]_2Ga[(CH_2)_3NEt_2]$	4	254.6(1)	[1b]
$Cp(CO)Ni\text{-}GaNp_2(THF)$	4	240.6(1)	[18]
$[(CO)_4Co]_2Ga[(2,6\text{-}Me_2NCH_2)2C_6H_3]$	5	257.2(2)	[19]

[*] This work.

lar solvents only, preferably in THF, but also in methylene chloride. The heterodinuclear complexes were separated from the alkali chloride as the only by-product by extraction into pentane, toluene, or methylene chloride. Trinuclear complexes with two different transition metal fragments bound to the gallium center were obtained by similar methods. Surprisingly, not every combination of metal fragments could be arranged around the gallium center so far. No reaction was observed for the combinations of **5a** (FeGa) with $Na[Mn(CO)_5]$ or **4e** (MnGa) and its cobalt analog with the respective transition metal carbonylates under the very same conditions which had previously afforded the symmetrically disubstituted species, e.g. **4f** (Mn_2Ga) or its cobalt analog[1b]. However, we were able to isolate **4g** (MnGaRe) from the reaction of **4e** with $Na[Re(CO)_5]$. But the related reaction of **3a** with $K[Cp(CO)_2Fe]$ did not give a pure product. This chemistry of mixed transition metal gallium complexes is currently under further investigation. Ion pair effects are important in these salt elimination reactions. Their success depends strongly on the nucleophilicity of the carbonyl metallate and the type of the counterion[20]. With non-coordinating counterions, e.g. $[R_4Z]^+$ (R = alkyl, aryl; Z = N, P, As), rather than with Na^+ or K^+, the monovalent carbonyl metallates did not give the M–Ga substitution products. Similar "inverse" salt effects were investigated for related alkylation reactions of some of the carbonyl metallates[20]. The new compounds **1a**–**7c** are soluble in all common aprotic organic solvents. With the exception of the hydrido derivatives **4b**, **5b**–**c**, **6b**, **6f**, **6h**, and the PPh_3-substituted compounds **6n**–**p**, they melt and sublime

Scheme 1. Synthesis of the complexes of type **1**–**7**

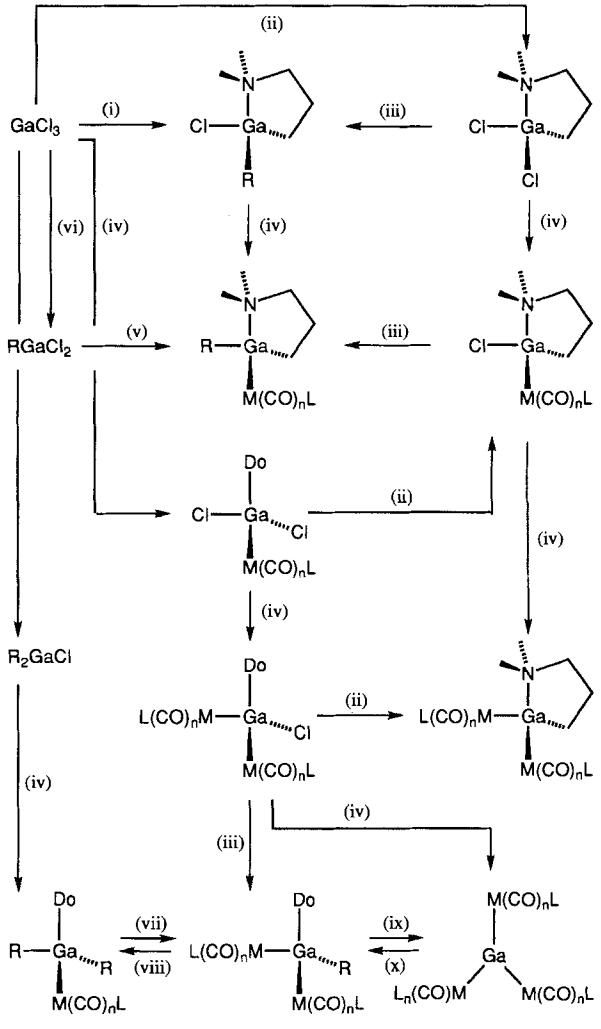

(i) 1. R_4Si; 2. $Li[(CH_2)_3NMe_2]$, Et_2O. – (ii) $Li[(CH_2)_3NMe_2]$, Et_2O, 25 °C. – (iii) R = alkyl, aryl: RLi, toluene; R = H: $Li[BEt_3H]$, THF; R = BH_4: $Li[BH_4]$, Et_2O. – (iv) $L(CO)_nM](Na/K)$; L = CO: toluene, pentane; L = Cp, PR_3: THF, Et_2O. – (v) R = H, alkyl: 1. $Li[(CH_2)_3NMe_2]$, pentane; 2. $[L(CO)_nM](Na/K)$. – (vi) Me_3SiH. – (vii) – $DoGaR_3$. – (viii): $+DoGaR_3$. – (ix): $-DoGa[M]R_2$. (x) $+DoGa[M]R_2$, +Do.

in vacuo without decomposition. The Cr–Ga complexes are rather light-sensitive in solution.

The chemical properties of **1a**–**7c** are characterized by the strong polarity of the M–Ga bonds being rapidly cleaved by electrophilic or nucleophilic attack, which we have previously exemplified by the chemistry of $(CO)_4Co\text{–}Ga(Np)_2(THF)$[1a]. This reactivity expectedly decreases with increasing nucleophilicity of the transition metal fragment and with the number of electronegative substituents at the gallium center. For example, the compound **5a** can be handled in air for a short period of time without decomposition, while compound **1b** decomposes instantaneously under the same conditions. The typical hydrolysis products are either transition metal carbonyl hydrides and oligomeric alkylgallium oxides[1a] or transition metal-substituted galloxanes, e.g. $(\mu\text{-}O)[(CO)_5Mn\text{–}Ga(\eta^1\text{-}2,4,6\text{-}tBu_3C_6H_2)]_2$[11].

Within seconds the M–Ga bonds are oxidatively cleaved by iodine to give the corresponding transition metal carbonyl iodides. Similar, but much slower reactions have been kinetically studied in detail for transition metal group 14 compounds[21].

In solution, three-fold coordinated gallium centers with a R_2Ga unit are usually not stable at a $L(CO)_nM$ fragment (Schemes 1 and 2). This is shown for example by the thermal conversion of $(CO)_4Co-Ga(Np)_2(PMc_3)$ into a mixture of different CoGa species[1a]. Such ligand redistribution reactions can be somewhat diminished by steric shielding of the metal centers as shown by some entries of Table 1. However, these compounds are not volatile unchanged. According to Scheme 2 the treatment of the intramolecularly adduct-stabilized compounds **6d–g** with the alkylphosphanes PR_3 (R = CH_3, C_2H_5) in pentane at −78 °C gave temp.-sensitive (> −20 °C) phosphane adducts as white microcrystalline solids. In a closed system (sealed NMR tube, [D_8]toluene) an equilibrium was observed between gallium-coordinated and free phosphane (^{31}P-NMR analysis). Upon warming to 80 °C reversible thermal decarbonylation occurred, which was accompanied by coordination of the phosphane at the cobalt center and recoordination of the amine donor. The *trans*-phosphane-substituted complexes **6k–t** were isolated in an open system (liberation of CO). In the case of sterically more demanding phosphanes (PCy_3, PPh_3) the gallium-coordinated phosphane intermediates were not detected spectroscopically. Apparently, chelate stabilization completely blocks alkyl exchange reactions. Also the other (not intramolecularly) donor-stabilized systems proved to be rather inert against alkyl exchange reactions at the gallium center when heated up to 150 °C in a sealed NMR tube. These results show, that steric and coordinative saturation at the gallium atom kinetically stabilizes alkylgallium transition metal complexes against otherwise facile alkyl redistribution reactions. The halide-functionalized compounds are generally much more resistant to ligand exchange than their alkyl congeners. Also the mixed metal system **4g** did not show a significant tendency to ligand exchange reactions at the gallium center.

The halide functions $GaCl_n$ (n = 1, 2) were selectively replaced by various residues (Schemes 1 and 3). The treatment of the transition metal carbonylates gave the trinuclear complexes **4f–g** and **6h**. The introduction of alkyl groups or other groups is possible without cleavage of the M–Ga bond. The reaction of $Cp(CO)_2Fe-GaCl_2(NMe_3)$ (**5a**) with two equivalents of KO*t*Bu in Et_2O gave colorless to pale yellow crystal plates of **5d**. The analytical data are consistent with the structure outlined in Scheme 3. The amine ligand was liberated and intermolecular dimerization occurred. A distinction between a *cis* and a *trans* configuration of the iron fragments at the Ga_2O_2 ring is currently not possible. The NMR spectra of **5d** show two different resonances for the *tert*-butyl substituents (Table 6). A similar structure type was observed for other sytems such as $[(CO)_3Ni-Ge(OtBu)]_2$[22]. The hydride species $Cp(CO)_2FeGa[(CH_2)_3NMe_2](H)$ (**5c**, or d_1-**5c**) were quantitatively

Scheme 2

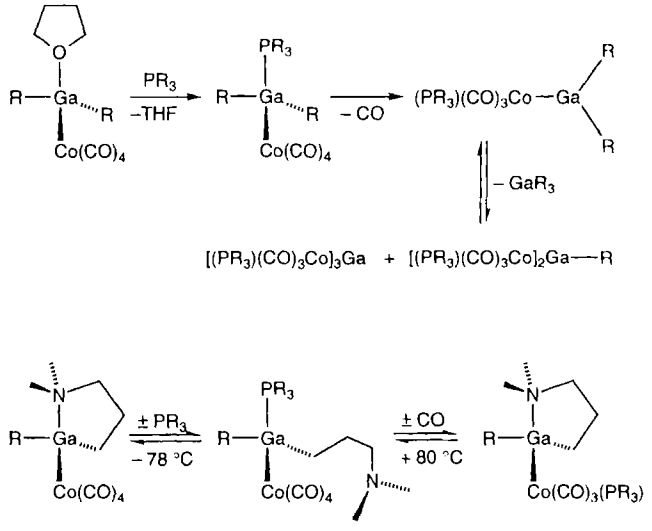

derived from **5e** with "Super-Hydride®", $Li[BEt_3H]$, in Et_2O without Fe–Ga bond cleavage or attack of the carbonyl groups.

Scheme 3

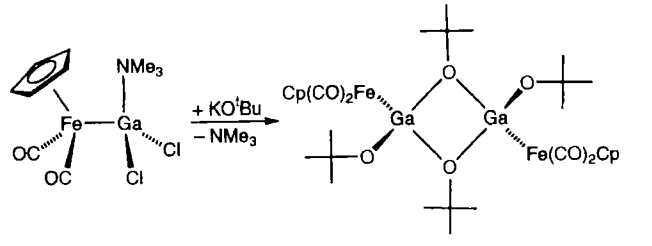

B. Spectroscopic Characterization

ν(CO)-IR Spectra

In non-polar, non-coordinating solvents (CCl_4, toluene, pentane, hexane, etc.) the complexes of the type $L(CO)_nM-Y$, with a local C_s symmetry at the metal show the expected ν(CO) bands in the IR spectra (Table 2). The mixed substituted compounds, e.g. **1b–3b**, exhibit a chiral gallium center. Thus, the symmetry is lowered to C_1 and the IR spectra may show more bands. For example, the usual pattern $2A_1$ + E for $(CO)_4Co-L$ complexes with local C_{3v} symmetry is reduced to C_s for **6a–c**. The spectra show split E bands. The relative intensity of the A_1 bands is increased for the C_1 systems **6d–h** compared to similar but achiral complexes. The ν(Ga–H) IR absorptions of **4b**, **5b–c**, **6b**, **6f** are observed as very broad bands at 1850–1910 cm^{-1}, which partly overlap with the ν(CO) absorptions. Deuteration gives rise to ν(Ga–D) absorptions of 1340 cm^{-1} (**5c**; calcd. 1310) and 1350 (**4b**: calcd. 1340). According to the IR spectra of either the reaction solutions or the pure complexes, isocarbonyl structures, e.g. M–CO–Ga, are absent. Depending on the polarity of the solvent, the transition metal fragment and the substitution patterns at both metals, more or less extensive metal-metal

bond heterolysis is observed. The two Co–Ga complexes $L(CO)_3Co-Ga[(CH_2)_3NEt_2](Cl)$ (**6v**: L = CO; **6s**: L = PPh_3) are typical examples. The extent of dissociation follows the relative nucleophilicity of the transition metal carbonylate in the respective solvent[23]. For example, the dissociation constants of the Lewis acid-base adducts $[L(CO)_nM-Ga(C_6H_5)_3]^-$ range over several orders of magnitude in dichloromethane: $(CO)_5Mn < (CO)_4Co < Cp(CO)_3W < (PR_3)(CO)_3Co < Cp(CO)_2Fe \approx Cp(CO)Ni$[24]. A trans-donor ligand to the gallium substituent at the cobalt center drastically lowers the tendency to dissociate. The characteristic absorptions for the free anion $[(Ph_3P)Co(CO)_3]^-$ (1900 and 1839 cm^{-1}) are absent in THF or acetonitrile solution (Figure 1). These results suggest, that the M–Ga bonds are best described by using a polar donor-acceptor model. Solvents with a high dielectric constant or a high donor ability promote heterolysis of the bond. Highly nucleophilic metal fragments efficiently compete with the solvent and the M–Ga bonds are stable. A second measure of the extent of the "polarity" of M–Ga bonds may be obtained by a comparison of the difference of the ν(CO) absorptions of the non-complexed metal carbonylate fragment and the respective values for the undissociated M–Ga complex. The shift to higher energy, $\Delta\nu(CO)^{as}$, of the symmetric $^{12}C-O$ stretching vibration resulting from complex formations was used as a sensitive measure of the acceptor strength of Lewis acids for the base $[(\eta^5-C_5H_5)(CO)_2Fe^-]$ [$\nu(CO)^{as}$ = 1770 cm^{-1}[25]]. For the gallium compounds $(\eta^5-C_5H_5)(CO)_2Fe-Ga[(CH_2)_3NMe_2](R)$ (R = Cl, Et) $\Delta\nu(CO)^{as}$ equals 130–150 cm^{-1}, while for $[(\eta^5-C_5H_5)(CO)_2Fe-E(C_6H_5)_3]^-$ $\Delta\nu(CO)^{as}$ amounts to 90 cm^{-1} if E = Al, Ga, and In, but to 139 cm^{-1} if E = B[24]. From this it may be concluded, that the σ(Fe–Ga) bonds of **5a–d** are clearly more covalent and less polarized than in the negatively charged Lewis acid/base adduct mentioned above. Typical covalent Fe–X bonds like in the systems $(\eta^5-C_5H_5)(CO)_2Fe-R$ (R = alkyl, stannyl) exhibit $\Delta\nu(CO)^{as}$ around 170 cm^{-1}, which is close to the value of 164 cm^{-1} of the $Fe-GaCl_2$ complex **5a**. In contrast to this, the respective values of $(\eta^5-C_5H_5)(CO)_2Fe-BR_2$ (R = C_6H_5; catecholate) are 180–200 cm^{-1}, which was attributed to significant Fe-B *multibonding*[26]. Another comparison is possible with the actinoide transition metal bonds of the type $(\eta^5-C_5H_5)(CO)_2M-An(X)(\eta^5-C_5H_5)_2$ (M = Fe, Ru; An = Th, U; X = Cl, CH_3, $\eta^5-C_5H_5$). Depending on the substituent X, the $\nu(CO)^{as}$ values can be as low as 1873 cm^{-1} [$\Delta\nu(CO)^{as}$ around 100 cm^{-1}] due to much more ionic M–An bonds. From this point of view the polarity of the M–Ga bonds **5a–d** is even more pronounced compared to the heterodinuclear "early-late" transition metal compounds of the type $[H_3CC(CH_2NSiMe_3)_3]Ti-Fe(CO)_2(\eta^5-C_5H_5)$[27] and $(\eta^5-C_5H_5)(RN)M-Fe(CO)_2(\eta^5-C_5H_5)$[28] [$\Delta\nu(CO)^{as} \approx 146 (\pm 5)$ cm^{-1}].

NMR Spectra

The chirality of the intramolecularly adduct-stabilized complexes of the general formula $L(CO)_nM-Ga[(CH_2)_3-NMe_2](R)$ causes complex multiplets in the ^{1}H-NMR spectra for the diastereotopic hydrogen atoms of the heterocycle (spin systems AA'BB' and AA'BB'CC') and the methylene groups or the methyl substituents at the nitrogen atom. The assignments given in the experimental part was confirmed by two-dimensional routine techniques (^{1}H-COSY and ^{1}H/^{13}C COSY). In the case of very nucleophilic transition metal centers (e.g. trans phosphane substituents) and bulky substituents R, especially the ^{1}H-NMR spectra are more complex due to dynamic effects. The Ga–N bond is weakened in these cases and the inversion at the nitrogen atom causes linebroadening and coalescence effects. At lower temp., typically below −30 °C, those dynamic effects were frozen. The persistance of a Cr–Ga bond, for example, and the absence of isocarbonyl structures Cr–CO–Ga in solution are nicely exemplified by the ^{13}C-NMR spectrum of **1b**. Three different resonances of almost equal intensity are observed for the *trans* carbonyl and the two diastereotopic *cis* carbonyl substituents at the chromium center in the expected range between 237.7 and 239.9 ppm (Tables 3–6).

Figure 1. Solvent dependency of the ν(CO)-IR spectra of $L(CO)_3-Co-Ga[(CH_2)_3NEt_2](Cl)$ (**I**: L = CO; **II**: L = PPh_3)[a]

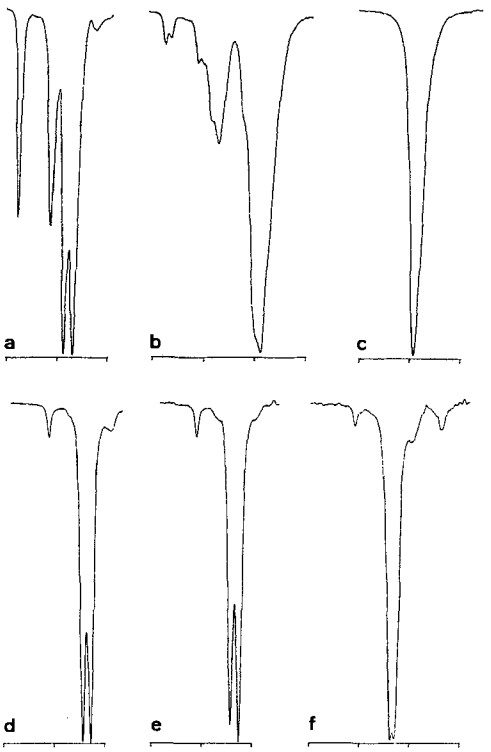

[a] **I**: a) *n*-Pentane (range: 2100–1900 cm^{-1}); – b) THF (range: 2100–1800 cm^{-1}); – c) acetonitrile (range: 2000–1800 cm^{-1}). – **II**: – d) toluene (range: 2100–1900 cm^{-1}); – e) THF (range: 2100–1900 cm^{-1}); f) acetonitrile (range: 2100–1800 cm^{-1}).

Mass Spectra

The compounds $L(CO)_nM-Ga[(CH_2)_3NMe_2](R)$ (R = alkyl) do not show the molecular peak in resonable quantities under EI, FI, or CI conditions (ca. 1% rel. int.). Cleavage of the M–Ga bond is preferred and the spectra are

Table 2. Infrared ν(CO) data and numbering scheme of the new compounds of the type $L(CO)_nM-GaR_2(Do)$ and $L(CO)_nM-Ga[(CH_2)_3NR']R$ [R = H, Cl, alkyl, $L(CO)_nM$; R' = Me, Et; L = Cp, PR_3, CO; n = 1, 2, 3, 4]

Compound	*No.*	*R*	*ν(CO)*
$Cp(CO)_3Cr-GaCl_2(NMe_3)$	**1a**		1984 vs 1915 sh 1898 vs[a]
$Cp(CO)_3Mo-GaCl_2(NMe_3)$	**2a**		2001 vs 1927 s 1909 vs[b]
$Cp(CO)_3W-GaCl_2(NMe_3)$	**3a**		1997 vs 1919 vs 1901 vs[b]
$Cp(CO)_3Cr-Ga[(CH_2)_3NMe_2](Cl)$	**1b**	Cl	1972 vs 1899 vs 1869 vs[b]
$Cp(CO)_3Mo-Ga[(CH_2)_3NMe_2](Cl)$	**2b**	Cl	1985 vs 1902 s 1880 vs[b]
$Cp(CO)_3W-Ga[(CH_2)_3NMe_2](Cl)$	**3b**	Cl	1980 vs 1898 vs 1872 vs[a]
$Cp^*(CO)_3Mo-Ga[(CH_2)_3NMe_2](Cl)$	**2b***	Cl	1978 s 1902 s 1878 s[d]
$Cp^*(CO)_3W-Ga[(CH_2)_3NMe_2](Cl)$	**3b***	Cl	1968 s 1887 s 1865 s[d]
$(CO)_5Mn-GaR_2(NMe_3)$	**4a**	Cl	2099 m 2034 m 2004 vs 1986 sh[b]
	4b	H	2097 w 2016 vs 2008 vs 1984 m[b]
	4c	Et	2066 s 2011 m 1981 sh 1956 vs[b]
$(CO)_5Mn-GaR_2(C_7H_{13}N)$	**4d**	Et	2065 s 2010 m 1980 sh 1957 vs[b]
$(CO)_5Mn-Ga[(CH_2)_3NMe_2](R)$	**4e**	Cl	2087 m 2015 m 1977 vs[b]
$[(CO)_5Mn]_2Ga[(CH_2)_3NMe_2]$	**4f**		2086 m 2059 m 2016 s 2000 m 1980 vs 1962 s[d]
$[(CO)_5Mn][(CO)_5Re]Ga[(CH_2)_3NMe_2]$	**4g**		2100 m 2061 s 2016 s 1985 vs 1966 s 1959 s[d]
$Cp(CO)_2Fe-GaR_2(NMe_3)$	**5a**	Cl	1989 vs 1934 vs[b]
	5b	H	1945 vs 1885 vs[e]
$Cp(CO)_2Fe-Ga[(CH_2)_3NMe_2](R)$	**5c**	H	2016 w* 1960 vs 1920 vs[e]
$Cp(CO)_2Fe-GaR_2$	**5d**	O^tBu	1985 vs 1936 vs[b]
$(CO)_4Co-GaR_2(NMe_3)$	**6a**	Cl	2093 s 2068 w* 2032 s 2007 vs 1989 vs[b]
	6b	H	2074 s 2006 s 1980 vs 1964 vs[d]
	6c	Et	2064 s 2028 w* 1997 s 1966 vs 1943 vs[d]
$(CO)_4Co-Ga[(CH_2)_3NMe_2](R)$	**6d**	Et	2065 s 1996 s 1966 vs 1955 vs[b]
	6e	Np	2066 s 1997 s 1967 vs 1955 vs[d]
	6f	H	2071 s 2004 s 1973 vs 1960 vs[d]
$(CO)_4Co-Ga[(CH_2)_3NEt_2](^tBu)$	**6g**	^tBu	2064 s 1997 s 1965 vs 1954 vs[d]
$[(CO)_4Co]_2GaH(THF)$	**6h**		2086 s 2064 s 2012 m 2009 s 1997 vs 1973 vs 1960 s[d]
$(PMe_3)(CO)_3Co-GaCl_2(NMe_3)$	**6i**		2084 w* 2024 w* 1992 m 1953 vs 1940 vs[b]
$(PMe_3)(CO)_3Co-Ga[(CH_2)_3NMe_2](R)$	**6k**	Cl	2014 w 1945 vs 1928 vs 1944 vs 1927 vs[b]
$(PMe_3)(CO)_3Co-Ga[(CH_2)_3NEt_2](R)$	**6m**	^tBu	1993 w 1922 vs 1907 vs[d]
$(PPh_3)(CO)_3Co-Ga[(CH_2)_3NMe_2](R)$	**6n**	Cl	2010 w 1946 vs 1925 vs[b]
	6p	^tBu	1929 vs 1914 vs[b]
$(PCy_3)(CO)_3Co-Ga[(CH_2)_3NEt_2](R)$	**6q**	Me	1986 w 1914 vs 1898 vs[d]
$(PEt_3)(CO)_3Co-Ga[(CH_2)_3NEt_2](R)$	**6r**	Me	1992 w 1906 vs 1920 vs[d]
$(PPh_3)(CO)_3Co-Ga[(CH_2)_3NEt_2](R)$	**6s**[†]	Cl	2010 w 1946 vs 1925 vs[b]
	6t	Me	1929 vs 1941 vs[d]
$(CO)_4Co-Ga[(CH_2)_3NEt_2](R)$	**6v**[†]	Cl	2083 s 2018 s 1991 vs 1976 vs[d]
	6w[†]	Me	2066 s 1998 s 1967 vs 1955 vs[d]
$Cp(CO)Ni-GaR_2(NMe_3)$	**7a**	Cl	2007 vs[c]
$Cp(CO)Ni-Ga[(CH_2)_3NEt_2](R)$	**7b**	Cl	1977 vs[b]
	7c	^tBu	1947 vs[b]

ν(CO)-IR data were obtained in solution between CaF_2 plates; solvents: [a] THF. – [b] Toluene. – [c] CH_2Cl_2. – [d] *n*-Pentane (*n*-hexane). – [e] Et_2O. – [*] Impurity. – [†] This compound has been published previously, see ref.[1b].

dominated by the stable dialkylgallium fragments $\{Ga[(CH_2)_3NMe_2](R)^+\}$ (base peak). The fragmentation of **6c** was studied with a high-resolution Fourier-transform ion cyclotron resonance mass spectrometer[29]. Cleavage of metal-ligand bonds efficiently competes with the Co–Ga bond fragmentation. The particle $[CoGa]^+$ was detected with roughly 30% relative intensity compared to the base peak $[GaEt_2]^+$. The observed fragments indicate the importance of homogeneous intramolecular β-H elimination processes during the decomposition of **6c** because fragments like $[(CO)_nCoGa(H)Et]^+$ were also detected. The ion $[CoGaH]^+$ (*m/z*: 129) was also observed. For $(CO)_4Co-Ga(Np)_2(THF)$ this low-energy fragmentation pathway is blocked. This may explain the rather different fragmentation pattern which is dominated by $[Ga(CH_2tBu)_2]^+$ and the missing of $[CoGa]^+$ in the respective spectra. Compounds of the type $L(CO)_nM-Ga[(CH_2)_3NMe_2](X)$ (X = Cl, $L(CO)_nM$) did not show such a preferred M–Ga bond cleavage. In the case of the Cr–Ga compound **1a** the molecular ion *m/z* = 393 (12% rel. int.) was clearly detected.

C. Structure

Molecular Structures of $(PPh_3)(CO)_3Co-Ga[(CH_2)_3NEt_2](R)$ (6s: R = Cl; 6t: R = CH_3). – Variation of σ(Co–Ga) Bond Lengths

The results of the single-crystal X-ray diffraction studies of **6s–t** are summarized in Tables 8 and 9. The molecular structures of **6s–t** are shown in Figures 2 and 3. The distorted tetrahedral coordination geometry at the gallium center and the trigonal-bipyramidal environments of the cobalt atoms in **6s–t** are rather similar to other Co–Ga compounds with a four-fold coordinated gallium atom (which were referred to in Table 1). In both cases the 3-(dimethylamino)propyl chelate ligand is disordered. The disorder of **6t** was resolved for C7/C97, C10/C90, C11/C91, C12/C92, and C13/C93 (Figure 3b). The positions N1, C5, and C6 are not significantly disordered. The disorder causes geometric

Table 3. Elemental analysis of the new compounds **1a–7c** ($R^1 = [(CH_2)_3NMe_2]$; $R^2 = [(CH_2)_3NEt_2]$)

		Analytical data(%); found (calcd.)					
Compound	*No.*	*C*	*H*	*N*	*Cl*	*Ga*	*M*
$Cp(CO)_3Cr\text{-}GaCl_2(NMe_3)$	**1a**	33.01	3.42	3.38		16.85	
$C_{11}H_{14}Cl_2CrGaNO_3$		(32.96)	(3.52)	(3.49)		(17.39)	
$Cp(CO)_3Mo\text{-}GaCl_2(NMe_3)$	**2a**	29.55	3.08	2.61	16.57	15.44	21.54
$C_{11}H_{14}Cl_2GaMoNO_3$		(29.70)	(3.17)	(3.15)	(15.94)	(15.67)	(21.57)
$Cp(CO)_3W\text{-}GaCl_2(NMe_3)$	**3a**	24.73	2.63	2.52		12.50	34.83
$C_{11}H_{14}Cl_2GaNO_3W$		(24.80)	(2.65)	(2.63)		(13.09)	(34.51)
$Cp(CO)_3Cr\text{-}GaR^1Cl$	**1b**	39.85	4.39	3.58	17.58	16.85	12.03
$C_{13}H_{17}ClCrGaNO_3$		(39.79)	(4.37)	(3.57)	(17.69)	(17.39)	(12.97)
$Cp(CO)_3Mo\text{-}GaR^1Cl$	**2b**	35.89	3.77	3.01			
$C_{13}H_{17}ClGaMoNO_3$		(35.78)	(3.93)	(3.21)			
$Cp^*(CO)_3Mo\text{-}GaR^1Cl$	**2b***	42.46	5.14	2.67			
$C_{18}H_{27}ClGaMoNO_3$		(42.68)	(5.37)	(2.77)			
$Cp(CO)_3W\text{-}GaR^1Cl$	**3b**	29.75	3.41	2.81	7.63		34.91
$C_{13}H_{17}ClGaNO_3W$		(29.78)	(3.27)	(2.67)	(6.76)		(35.07)
$Cp^*(CO)_3W\text{-}GaR^1Cl$	**3b***	36.55	4.69	2.35	5.83		31.32
$C_{18}H_{27}ClGaNO_3W$		(36.37)	(4.58)	(2.36)	(5.96)		(30.93)
$(CO)_5Mn\text{-}GaCl_2(NMe_3)$	**4a**	23.05	2.31	3.30	19.72	18.58	13.50
$C_8H_8Cl_2GaMnNO_5$		(24.34)	(2.30)	(3.55)	(17.96)	(17.66)	(13.92)
$(CO)_5Mn\text{-}GaH_2(NMe_3)$	**4b**	29.02	3.05	3.93			
$C_8H_{11}GaMnNO_5$		(29.49)	(3.40)	(4.30)			
$(CO)_5Mn\text{-}GaEt_2(NMe_3)$	**4c**	37.40	5.02	3.28			18.79
$C_{12}H_{19}GaMnNO_5$		(37.74)	(5.01)	(3.67)			(14.38)
$(CO)_5Mn\text{-}GaEt_2(NC_7H_{13})$	**4d**	44.19	5.56	3.29		15.95	12.44
$C_{16}H_{23}GaMnNO_5$		(44.28)	(5.34)	(3.23)		(16.06)	(12.66)
$(CO)_5Mn\text{-}GaR^1Cl$	**4e**	30.97	3.46	3.67			
$C_{10}H_{12}ClGaMnNO_5$		(31.09)	(3.13)	(3.63)			
$[(CO)_5Mn]_2GaR^1$	**4f**	32.72	2.38	2.59			
$C_{15}H_{12}GaMn_2NO_{10}$		(33.01)	(2.22)	(2.57)			
$[(CO)_5Mn][(CO)_5Re]GaR^1$	**4g**	25.74	1.90	2.06			28.66
$C_{15}H_{12}GaMnReNO_{10}$		(26.61)	(1.79)	(2.07)			(27.50)
$Cp(CO)_2Fe\text{-}GaCl_2(NMe_3)$	**5a**	31.61	3.68	3.59			
$C_{10}H_{14}Cl_2FeGaNO_2$		(31.89)	(3.75)	(3.72)			
$Cp(CO)_2Fe\text{-}Ga(O^tBu)_2$	**5d**	43.57	5.59			17.23	15.84
$C_{15}H_{23}FeGaO_4$		(45.85)	(5.90)			(17.74)	(14.21)
$(CO)_4Co\text{-}GaCl_2(NMe_3)$	**6a**	22.88	2.68	3.79		18.47	14.54
$C_7H_9Cl_2CoGaNO_4$		(22.68)	(2.45)	(3.78)		(18.81)	(15.90)
$(CO)_4Co\text{-}GaH_2(NMe_3)$	**6b**	27.54	3.48	4.44			
$C_7H_{11}CoGaNO_4$		(27.86)	(3.67)	(4.64)			
$(CO)_4Co\text{-}GaEt_2(NMe_3)$	**6c**	36.82	5.23	3.77		19.10	15.95
$C_{11}H_{19}CoGaNO_4$		(36.91)	(5.35)	(3.91)		(19.48)	(16.46)
$(CO)_4Co\text{-}GaR^1(Et)$	**6d**	36.92	4.77	3.84		19.01	16.14
$C_{11}H_{17}CoGaNO_4$		(37.12)	(4.81)	(3.94)		(19.59)	(16.56)
$(CO)_4Co\text{-}GaR^1(Np)$	**6e**	42.72	6.30	3.70		17.80	12.60
$C_{14}H_{23}CoGaNO_4$		(42.25)	(5.82)	(3.52)		(17.52)	(14.81)
$(CO)_4Co\text{-}GaR^1H$	**6f**	32.56	3.75	4.04			
$C_9H_{13}CoGaNO_4$		(32.97)	(4.00)	(4.27)			
$(CO)_4Co\text{-}GaR^2(^tBu)$	**6g**	43.47	6.02	3.17		16.40	13.95
$C_{15}H_{25}CoGaNO_4$		(43.73)	(6.12)	(3.40)		(16.92)	(14.30)
$[(CO)_4Co]_2GaH(THF)$	**6h**	29.25	1.66			13.95	24.0
$C_{12}H_9Co_2GaO_9$		(29.73)	(1.87)			(14.38)	(24.31)
$(PMe_3)(CO)_3Co\text{-}GaCl_2(NMe_3)$	**6i**	24.74	4.25	2.64	17.52	15.99	13.31
$C_9H_{18}Cl_2CoGaNO_3P$		(25.81)	(4.33)	(3.34)	(16.93)	(16.65)	(14.07)
$(CO)_4Co\text{-}GaR^1(Cl)$	**6j**	29.84	3.34	3.87			
$C_9H_{12}ClCoGaNO_4$		(29.80)	(3.48)	(4.09)			
$(PMe_3)(CO)_3Co\text{-}GaR^1Cl$	**6k**	32.65	5.37	3.21			
$C_{11}H_{21}ClCoGaNO_3P$		(32.20)	(5.16)	(3.41)			
$(PMe_3)(CO)_3Co\text{-}GaR^2(^tBu)$	**6m**	44.05	7.53	2.96			
$C_{17}H_{34}CoGaNO_3P$		(44.38)	(7.45)	(3.04)			
$(PPh_3)(CO)_3Co\text{-}GaR^1(Cl)$	**6n**	52.31	4.68	2.26	5.87		
$C_{26}H_{27}ClCoGaNO_3P$		(52.34)	(4.56)	(2.35)	(5.94)		
$(PPh_3)(CO)_3Co\text{-}GaR^1(^tBu)$	**6p**	57.69	5.95	2.14			
$C_{30}H_{36}CoGaNO_3P$		(58.28)	(5.87)	(2.27)			
$(PCy_3)(CO)_3Co\text{-}GaR^2(Me)$	**6q**	56.11	8.71	1.97			
$C_{29}H_{52}CoGaNO_3P$		(55.97)	(8.42)	(2.25)			
$Cp(CO)Ni\text{-}GaCl_2(NMe_3)$	**7a**	30.66	3.87	3.66	19.89		
$C_9H_{14}Cl_2GaNiNO$		(30.75)	(4.01)	(3.98)	(20.17)		
$Cp(CO)Ni\text{-}GaR^2(Me)$	**7b**	47.64	6.65	3.74			
$C_{14}H_{24}GaNiNO$		(47.98)	(6.90)	3.99			
$Cp(CO)Ni\text{-}GaR^2(^tBu)$	**7c**	51.56	7.56	3.44		17.20	14.28
$C_{17}H_{30}GaNiNO$		(51.98)	(7.70)	(3.57)		(17.75)	(14.94)

Table 4. ^{1}H-NMR data of the complexes of the type $L(CO)_nM-Ga[(CH_2)_2NR^1_2]R^2$

Compound	*No.*	*L*	*N-R*^{1}	$C^{\alpha}H_2$	$C^{\beta}H_2$	$C^{\gamma}H_2$	*Ga-R*^{2}
$Cp(CO)_3Cr-Ga[(CH_2)_3NMe_2]Cl$	**1b**	4.32 (s, 5H)	1.89 (s, 3H) 2.35 (s, 3H)	0.99 1.19	1.57 1.71	1.84 2.13	
$Cp(CO)_3Mo-Ga[(CH_2)_3NMe_2]Cl$	**2b**	4.84 (s, 5H)	1.97 (s, 3H) 2.37 (s, 3H)	0.91 1.10	1.55 1.71	1.89 2.11	
$Cp^*(CO)_3Mo-Ga[(CH_2)_3NMe_2]Cl$	**2b***	1.84 (s, 5H)	1.88 (s, 3H) 2.36 (s, 3H)	0.87 1.04	1.59 1.76	1.78 2.23	
$Cp(CO)_3W-Ga[(CH_2)_3NMe_2]Cl$	**3b**	4.79 (s, 5H)	1.87 (s, 3H) 2.18 (s, 3H)	0.87 1.09	1.72 1.79	1.87 2.18	
$Cp^*(CO)_3W-Ga[(CH_2)_3NMe_2]Cl$	**3b***	1.91 (s, 5H)	1.95 (s, 3H) 2.36 (s, 3H)	1.03 1.11	1.64 1.74	1.76 1.95	
$[(CO)_5Mn]_2Ga[(CH_2)_3NMe_2]$	**4f**		2.06 (s, 6H)	1.46	1.65	2.03	
$[(CO)_5Mn][(CH_2)_3NMe_2]Ga-[Re(CO)_5]$	**4g**		1.99 (s, 6H)	1.50	1.65	1.96	
$Cp(CO)_2Fe-Ga[(CH_2)_3NMe_2]H$	**5c**	4.24 (s, 5H)	1.90 (s, 3H) 2.36 (s, 3H)	0.85 1.07	1.28 1.35	1.86 2.15	6.04 (s, br, 1H)
$(CO)_4Co-Ga[(CH_2)_3NMe_2]H$	**6f**		1.90 (s, 3H) 2.01 (s, 3H)	0.88 0.93	1.47 1.57	1.76 1.98	5.65 (s, br, 1H)
$(CO)_4Co-Ga[(CH_2)_3NMe_2]CH_2{}^tBu$	**6e**		1.71 (s, 3H) 1.95 (s, 3H)	[*]			1.08 (s, 9H) [*]
$(CO)_4Co-Ga[(CH_2)_3NEt_2]{}^tBu$	**6g**		0.55 (m, 6H) 2.35 (m, 4H)	0.87 1.04	1.38 1.69	1.92 2.22	1.26 (s, 9H)
$(CO)_4Co-Ga[(CH_2)_3NMe_2]Cl$	**6j**		1.71 (s,3H) 2.11 (s,3H)	0.94 1.10	1.23 1.40	1.76 1.91	
$(PMe_3)(CO)_3Co-Ga[(CH_2)_3NMe_2](Cl)$	**6k**	1.02 (d, 9H)	2.41 (s, 3H) 1.97 (s, 3H)	1.16 1.21	1.50 1.70	1.85 2.35	
$(PMe_3)(CO)_3Co-Ga[(CH_2)_3NEt_2]({}^tBu)$	**6m**	1.01 (d, 9H)	0.61 (m, 3H) 0.73 (m, 3H) 3.02 (m, 1H) 2,50 (m, 2H)	1.06 1.20	1.01 1.93	2.01 2.05	1.47 (s, 9H)
$(PPh_3)(CO)_3Co-Ga[(CH_2)_3NMe_2](Cl)$	**6n**	7.53 6.95 (m, 15H)	2.36 (s, 3H) 2.07 (s, 3H)	1.09 1.19	1.46 1.61	1.76 2.24	
$(PPh_3)(CO)_3Co-Ga[(CH_2)_3NMe_2]({}^tBu)$	**6p**	7.70 7.02 (m, 15H)	2.21 (s, 3H) 2.12 (s, 3H)	1.07 1.23	1.71 1.84	1.98 2.05	1.46 (s, 9H)
$Cp(CO)Ni-Ga[(CH_2)_3NEt_2]{}^tBu$	**7c**	5.22 (s, 5H)	0.65 (t, 3H) 1.11 (q, 2H)	0.66 0.79	1.60 2.08	2.10 2.46	1.19 (s, 9H)
$Cp(CO)Ni-Ga[(CH_2)_3NEt_2]Me$	**7d**	5.88 (s, 5H)	0.58 (t, 3H) 0.80 (q, 2H)	0.64 0.93	1.61 1.65	2.11 2.38	0.25 (s, 3H)

[*] The explicit assignment is omitted because of extensive overlapping of broadened signals.

distortions of the C–C and C–N bond geometries in the case of freely refined atomic positions. The structural features of this part of **6t** however are very similar to the known structures of closely related systems[1f]. For this reason restrictions to fix the geometry were not applied to the structure solution of **6t**. The principal geometric parameters of **6t**, e.g. the entries of Table 8, proved to be not significantly affected by the disorder of the chelate ring. The same holds for compound **6s**. A very detailed analysis of the structural properties of **6s–t** is thus not justified. But we only want to discuss the trend of the Co–Ga bond lengths in a series of similar compounds. The measured Co–Ga lengths for **6s–t** are clearly reliable enough for this purpose. On the basis of covalent radii a σ(Co–Ga) single bond length may be estimated to be 248 (± 5) pm. The cubic intermetallic phase β-$Co_{0.50}Ga_{0.50}$ (CsCl structure)[1c] and the compound **6t** exhibit very similar Co–Ga contacts of 249.4(5) and 249.5(1) pm, respectively. For the heterodinuclear particle [CoGa] a triplet ground state with *d*(Co–Ga) = 250(5) pm and a dissociation energy of 2.33 eV (226 kJ · mol^{-1}) were found by ab initio calculations (density functional methods)[29]. σ(Co–Ga) bond lengths in molecular compounds can apparently vary over a wide range starting from 257.83(4) pm of $(CO)_4Co-Ga(CH_2t\text{-}Bu)_2(THF)$[1a] to the so far shortest contact of 237.8(1) pm of $(PPh_3)(CO)_3Co-Ga[(CH_2)_3NEt_2](Cl)$ (**6s**). Table 1 shows, that the coordination number exerts only a minor effect on the M–Ga bond lengths. The type of substituents at both metal centers is the more important factor. It should be mentioned that the W–Ga distance of 271 pm for $Cp(CO)_3W-Ga(CH_3)_2$ is significantly *larger* than the sum of the covalent radii, although the gallium is only three-fold coordinated. The shortening of the Co–Ga bond lengths of **6s–t** compared to $(CO)_4Co-Ga(CH_2t\text{-}Bu)_2(THF)$ cannot be caused by steric factors alone. This is indicated by the significant difference of 10 pm of the Co–Ga bonds of **6s** and **6t**, since the steric requirements of a methyl and chlorine substituent are not very different[30]. Given that short bonds may indicate stronger bonds in structurally similar systems, one may conclude that the Co–Ga dissociation energy of **6s–t** should be somewhat higher compared to $(CO)_4Co-GaR_2(Do)$. This is also indicated by significant amounts of the molecular ion in the EI-mass spectra of **6j–n** and the diminished tendency of **6k–n**

Table 5. $^{13}C\{^1H\}$-NMR data of the complexes of the type $L(CO)_nM-Ga[(CH_2)_3NR^1_2]R^2$

Compound	*No.*	*L*	*N-R¹*	$C^{\alpha}H_2$	$C^{\beta}H_2$	$C^{\gamma}H_2$	*Ga-R²*	*CO*
$Cp(CO)_3Cr-Ga[(CH_2)_3NMe_2]Cl$	**1b**	86.7	48.5	19.6	23.3	63.8		236.0 (cis)
		(C_5H_5)	44.8					237.7 (cis)
								239.9 (trans)
$Cp(CO)_3Mo-Ga[(CH_2)_3NMe_2]Cl$	**2b**	90.3	44.9	19.9	23.7	64.0		227.7 (cis)
		(C_5H_5)	48.5					228.8 (cis)
								230.5 (trans)
$Cp^*(CO)_3Mo-Ga[(CH_2)_3NMe_2]Cl$	**2b***	102.5	45.6	17.9	23.9	63.9		221.4 (cis)
		10.9	48.8					222.3 (cis)
		(C_5Me_5)						223.8 (trans)
$Cp(CO)_3W-Ga[(CH_2)_3NMe_2]Cl$	**3b**	88.5	45.0	20.0	24.0	64.5		218.2 (cis)
		(C_5H_5)	47.0					218.8 (cis)
								219.4 (trans)
$[(CO)_5Mn][(CH_2)_3NMe_2]Ga-[Re(CO)_5]$	**4g**		48.7	22.1	23.5	63.0		not observed
$[(CO)_5Mn]_2Ga[(CH_2)_3NMe_2]$	**4f**		47.6	22.2	22.9	63.1		not observed
$Cp(CO)_2Fe-Ga[(CH_2)_3NMe_2]H$	**5c**	81.7	48.8	14.9	24.8	64.2		219.7 (cis)
		(C_5H_5)	46.7					219.3 (cis)
								218.9 (trans)
$Cp(CO)_2Fe-Ga[(CH_2)_3NMe_2](O^tBu)$	**5e**	81.5	45.8	16.9	23.3	62.7	34.5 ($\underline{C}CH_3$)	217.7
		(C_5H_5)	46.5				69.5 ($\underline{C}Me_3$)	218.9
$(CO)_4Co-Ga[(CH_2)_3NMe_2](H)$	**6f**		48.0	14.8	23.8	65.6		203.5
			46.2					
$(CO)_4Co-Ga[(CH_2)_3NEt_2]^tBu$	**6g**		8.5 44.9	14.6	22.6	56.4	30.7 ($\underline{C}Me_3$)	204.4
			8.3 44.3				31.5 ($\underline{C}CH_3$)	
$(PMe_3)(CO)_3Co-Ga[(CH_2)_3NMe_2](Cl)$	**6k**	19.5	47.2	17.6	22.8	61.9		202.9 (d)
		(PCH_3)	43.9					[^2J(P,C) = 16 Hz]
$(PMe_3)(CO)_3Co-Ga[(CH_2)_3NEt_2](^tBu)$	**6m**	19.4	9.3 44.9	14.6	23.4	55.9	32.2 ($\underline{C}Me_3$)	206.6 (d)
		(PCH_3)	7.5 43.1				29.6 ($\underline{C}CH_3$)	[^2J(P,C) = 15 Hz]
$(PPh_3)(CO)_3Co-Ga[(CH_2)_3NMe_2](^tBu)$	**6p**	134.3	47.7	13.5	23.7	64.5	31.5 ($\underline{C}Me_3$)	206.0 (d, br)
		132.7	47.5				28.5 ($\underline{C}CH_3$)	[^2J(P,C) = 14 Hz]
		130.7						
		129.2						
		(PC_6H_5)						
$(PCy_3)(CO)_3Co-Ga[(CH_2)_3NEt_2](Me)$	**6q**	37.6	46.0 (br)	15.8	23.6	58.3	2.3	207.0 (d, br)
		30.4	8.7 (br)				(d, $GaCH_3$)	[^2J(P,C) = 16 Hz]
		28.3					[^3J(P,C) =	
		26.9					5.3 Hz]	
		(PC_6H_{11})						
$(PEt_3)(CO)_3Co-Ga[(CH_2)_3NEt_2](Me)$	**6r**	21.9	45.9 (br)	16.1	23.5	58.0	2.4	207.2 (d, br)
		8.1	8.6 (br)				(d, $GaCH_3$)	[^2J(P,C) = 16 Hz]
		(PC_2H_5)					[^3J(P,C) =	
							5 Hz]	
$Cp(CO)Ni-Ga[(CH_2)_3NEt_2]Me$	**7d**	89.0	9.3 45.0	15.5	23.3	57.6	3.1	194.0
			10.5 47.9					

Table 6. ^1H-NMR and $^{13}C\{^1H\}$-NMR data of the complexes of the type $L(CO)_nM-GaCl_2(Do)$

		^1H-NMR		*^{13}C-NMR*		
Compound	*No.*	*L*	*N-CH_3*	*L*	*N-CH_3*	*CO*
$Cp(CO)_3Cr-GaCl_2(NMe_3)$	**1a**	4.39 (s, 5H)	2.11 (s, 9H)	87.7	48.8	239.9 (trans)
						236.3 (cis)
$Cp(CO)_3Mo-GaCl_2(NMe_3)$	**2a**	4.81 (s, 5H)	2.12 (s, 9H)	91.0	48.4	231.0 (trans)
						227.5 (cis)
$Cp(CO)_3W-GaCl_2(NMe_3)$	**3a**	4.78 (s, 5H)	2.12 (s, 9H)	89.6	48.5	219.6 (br)
$(CO)_5Mn-GaCl_2(NMe_3)$	**4a**		2.00 (s, 9H)		46.8	[a]
$Cp(CO)_2Fe-GaCl_2(NMe_3)$	**5a**	4.93 (s, 5H)	2.69 (s, 9H)	83.5	48.3	215.6
$Cp(CO)_2Fe-Ga(O^tBu)_2$	**5d**	5.13 (s, 5H)	*Ga-O^{t}Bu:*	93.9	*O^{t}Bu:*	227.5 (trans)
			1.41 (s, 9H)		43.4	226.1 (cis)
			1.15 (s, 9H)		44.0	
					80.6	
					85.0	
$(CO)_4Co-GaCl_2(NMe_3)$	**6a**		2.05 (s, 9H)		47.8	[a]
$(PMe_3)(CO)_3Co-GaCl_2(NMe_3)$	**6i**	0,93 (s, 9H)	2.28 (s, 9H)	19.1	47.7	200.8
$Cp(CO)Ni-GaCl_2(NMe_3)$	**7a**	5.95 (s, 5H)	2.45 (s, 9H)	89.5	49.1	197.1

[a] The signal was not observed at room temperature.

Table 7. ^{1}H-NMR and ^{13}C{^{1}H}-NMR data of the compounds of the type $(CO)_nM-GaR_2(Do)$

		^{1}H-NMR		^{13}C-NMR		
Compound	No.	Do	Ga-R	Do	Ga-R	CO
$(CO)_5Mn-GaH_2(NMe_3)$	**4b**	1.92 (s, 9H)	5.49 (s, br, 2H)	49.3		219.8 [a]
$(CO)_5Mn-GaEt_2(NMe_3)$	**4c**	1.68 (s, 9H, br)	0.82 (d, br, 4H)	47.9	11.4	not
			1.37 (t, 6H)		10.0	observed
$(CO)_5Mn-GaEt_2(C_7H_{13}N)$	**4d**	2.53 (t. 6H, br)	0.87 (q, 4H)	47.5	11.5	not
		0.87 (d, 6H)	1.43 (t, 6H)	24.6	9.3	observed
		1.11 (m, 1H, br)		19.6		
$(CO)_4Co-GaH_2(NMe_3)$	**6b**	1.92 (s, 9H)	5.36 (s, br, 2H)	49.4		not
						observed
$(CO)_4Co-GaEt_2(NMe_3)$	**6c**	1.74 (s, 9H)	0.79 (q, 4H)	48.9	11.3	not
			1.34 (t, 6H)		10.8	observed
$[(CO)_4Co]_2GaH(THF)$	**6h**	3.55 (m, 4H)	6.23 (s, br, 1H)			
		1.03 (m, 4H)				

[a] [D$_8$]Toluene, −80 °C.

and **6s**−**t** to dissociate in polar solvents. These effects can be rationalized as follows. A strong σ-donor ligand *trans* to the gallium acceptor increases the σ-electron density at the cobalt center. The HOMO of a C_{3v}-symmetric d^{10}-$L(CO)_3Co^{(-)}$ fragment is mainly a metal d_{z^2}-type function and antibonding with respect to the σ(L−Co) bond[31]. A strong σ-donor pushes the HOMO of the metal fragment to higher energies. Electron withdrawing groups, e.g. halogen substituents, at the gallium center lower the energy of the LUMO of the $Ga^{(+)}$ moiety. Both effects favor the M−Ga bond formation by improving the energy match of the important interacting σ-orbitals. Comparably low-lying σ*(Ga−Cl)-acceptor orbitals may be also involved in this respect as will be discussed later. The variation of the acceptor strength of $GaR_2(Do)$-moieties (R = H, Cl, alkyl) in $(CO)_4Co$ complexes can also be deduced from the ν(CO)-IR absorptions as discussed above for Fe−Ga compounds. The values of the A_1 absorptions of the compounds $(CO)_4Co-GaR_2(NMe_3)$ range from 2093 cm^{-1} for R = Cl over 2083 cm^{-1} (R = H) to 2064 cm^{-1} (R = alkyl). The Lewis base Do at the gallium atom has only little influence. The series of phosphane derivatives behave similarly (Table 2). From this discussion it may be concluded, that the σ(Co−Ga) bond in $(Me_3P)(CO)_3Co-GaCl_2(NMe_3)$ (**6i**) could be even shorther than in **6s**. The structural characterization of **6i** is currently in progress.

Molecular Structure of $Cp(CO)_2Fe-GaCl_2(NMe_3)$ (5a)

Power et al. studied the Fe−Ga bonding properties of $Cp(CO)_2Fe-GatBu_2$, *d*(Fe−Ga) = 241.3 pm, which is one of the very few moderately stable diorganogallium transition metal compounds with a low-coordinated gallium center. However, Fe−Ga multiple bond effects were judged to be very small. The σ(Fe−Ga) bond lengths typically range around 245 pm (Table 1). From the study of the Co−Ga complexes **6s**−**t** we deduced, that the σ(Fe−Ga) bond length in **5a** should be shorter than that in compounds such as $Cp(CO)_2Fe-GatBu_2$. The results of a single-crystal X-ray structural analysis of **5a**, showing a short Fe−Ga contact of 236.18(3) pm, are in full agreement with

Figure 2. Molecular structure of $(PPh_3)(CO)_3Co-Ga[(CH_2)_3-NEt_2](Cl)$ (**6s**) in the crystal (SCHAKAL diagram [44])[a]

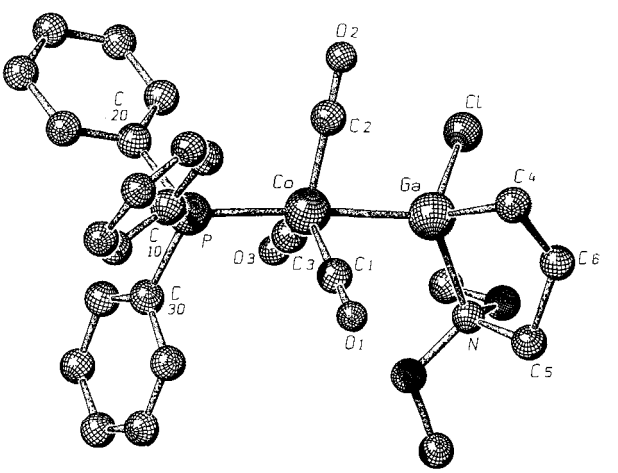

[a] Selected bond lengths [pm] and angles [°]: Co−Ga 237.78(4); Ga−Cl 217.6(1); Ga−N 217.2(3); Ga−C4 201.8(2); Co−Cl 176.0(3); Co−C2 177.2(3); Co−C3 175.6(3); Co−P 220.0(1); O1−Cl; 114.5(3); O2−C2 114.2(3); O3−C3 115.1(4); Ga−Co−P 175.6(1); Ga−Co−C1 84.4(1); Ga−Co−C2 83.5(1); Ga−Co−C3 83.7(1); Co−Ga−Cl; 114.50(3); Co−Ga−N 116.93(6); Co−Ga−C4 120.20(7); Cl−Ga−N 103.22(7); Cl−Ga−C4 101.06(9); N−Ga−C4 98.0(1).

this assumption. These findings agree with the known fact, that transition metal main-group metal bond lengths are very sensitive to variations of the group electronegativity of the metal fragments. The molecular structure of **5a** is shown in Figure 4. The sum of the covalent radii of Ga (125 pm) and Fe (126 pm) amounts to roughly 250 pm. The dative Ga−N bond of 209 pm is rather short compared with other alkylgallium compounds, e.g. in $Me_3Ga-NMe_3$ with 220(3) pm[32] or in 1-galla-5-azabicyclo[3.3.3]undecane with 209.5(2) pm[33], which reflects the enhanced acceptor strength of the $GaCl_2$ unit compared with the dialkylgallium moieties. The angles OC−Fe−Ga show a weak tendency. Complexes with long Fe−Ga bonds and a rather pronounced negative charge of the carbonyl substituents (IR) exhibit the smallest angles close to 80°[1f]. The com-

pound **5a** with the so far shortest Fe–Ga bond shows the largest angle of 92°. This variation of the OC–Fe–Ga angles probably reflects the variation of the negative charging of the $Cp(CO)_2Fe$ fragment similar to some Fe–In and Ni–In congeners[34]. Terminal Ga–Cl bond lengths of four-fold coordinated gallium compounds typically range around 216 (± 5) pm (see the Cambridge Structural Database, e.g. Me_3PGaCl_3, Ga–Cl: 217.4(4) pm[35]). The averaged Ga–Cl bond length of **5a** around 225 pm is thus comparatively long. This effect may be interpreted as a structural manifestation of some $Fe(d_\pi)\rightarrow\sigma^*(Ga-Cl)$ back donation. Similar effects have been thoroughly discussed for the $L_nM\rightarrow PX_3$ *π-acidic* back-bonding (X = F, H, alkyl)[36].

Figure 3a. Molecular structure of $(PPh_3)(CO)_3Co-Ga[(CH_2)_3NEt_2](CH_3)$ (**6t**) in the crystal (SCHAKAL diagram [44][a]

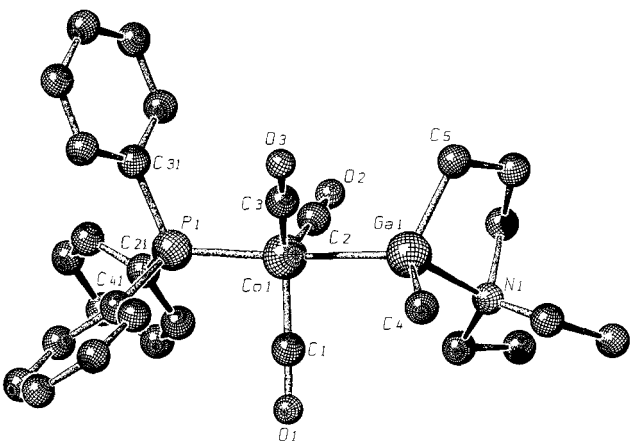

[a] Selected bond lengths [pm] and angles [°]: Co1–Ga1 249.5(1); Ga1–C4 195.5(7); Ga1–C5 197.1(7); Ga1–N1 215.2(6); Co1–C1 175.6(7); Co1–C2 173.9(7); Co1–C3 174.2(7); Co1–P1 218.8(2); O1–C1 113.8(8); O2–C2 114.1(7); O3–C3 115.2(8); Ga1–Co1–P1 170.8(1); Ga1–Co1–C1 86.1(2); Ga1–Co1–C2 87.8(2); Ga1–Co1–C3 75.8(2); Co1–Ga1–C5 113.4(2); Co1–Ga1–N1 117.6(2); Co1–Ga–C4 112.9(3); C5–Ga1–N1 88.9(3); C4–Ga1–C5 118.4(4); N1–Ga1–C4 103.4(3).

Figure 3b. Resolved disorder of the metallacyclic structure element of compound $(PPh_3)(CO)_3Co-Ga[(CH_2)_3NEt_2](CH_3)$ (**6t**) in the crystal (SCHAKAL diagram; the cobalt fragment has been omitted for clarity)

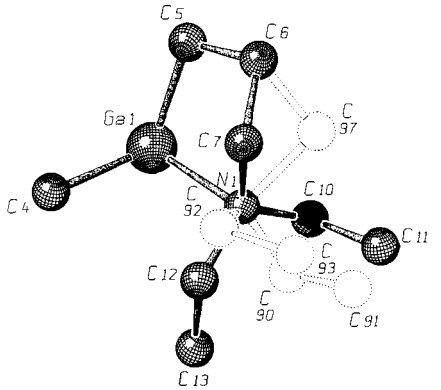

D. MOCVD

A selection of compounds exhibiting various metal combinations and stoichiometries were tested for their potential as single-source precursors for low-pressure MOCVD of intermetallic films. A study of the relationship between molecular structure of the precursor and thin film properties was recently presented for Fe/Ga[8] and Mn/Ga[23] films. In this paper we briefly describe the deposition of CoGa films. Figure 4 shows an AUGER spectra of the purest β-CoGa film grown from a single source to date. The 1:1 stoichiometry of the precursor **6c** is perfectly retained in the thin film above 300 °C substrate temp. (as confirmed by SEM-EDX and also by AAS after dissolution of the films in diluted nitric acid). Neither chelating alkyl ligands and hydride substituents at the gallium nor trans phosphane substitution at the cobalt center (**6d**, **6e**, **6f**, **6g**, **6m**) could improve the thin-film quality or the stoichiometry control. Halogen substituents (**6a**, **6i**, **6k**) which enhance the chemical stability of the precursor to some extent as discussed above, are however undesired, since they tend to end up as serious impurities in the films. It thus appears from our studies that as far as organometallic single molecule sources are concerned, compound **6c** is the best choice at present to deposit pure CoGa thin films.

Figure 4. Molecular structure of $(\eta^5\text{-}C_5H_5)(CO)_2Fe-GaCl_2[N(CH_3)_3]$ (**5a**) in the crystal (PLATON diagram[43], thermal ellipsoids are drawn at a 50% level)[a]

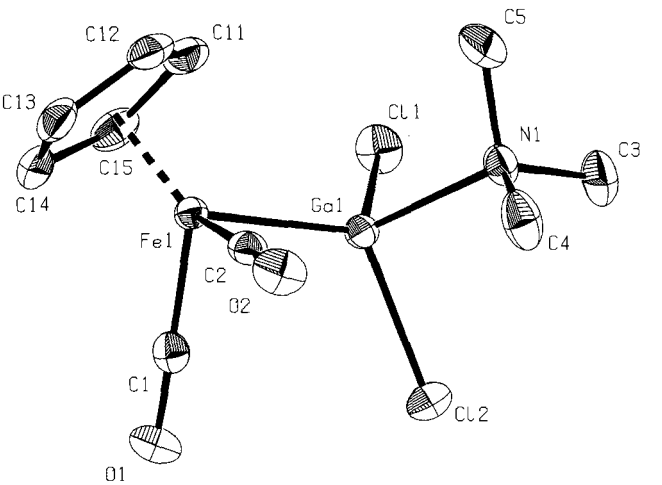

[a] Selected bond lengths [pm] and angles [°]: Fe1–Ga1 236.18(3); Ga1–Cl1 225.13(4); Ga1–Cl2 224.01(4); Ga1–N1 208.9(1); Fe1–C1 175.7(2); Fe1–C2 174.9(2); O1–C1; 114.8(2); O2–C2 115.1(2); Fe1–Ga1–N1 119.25(4); Fe1–Ga1–Cl1 116.77(1); Fe1–Ga1–Cl2 118.72(1); N1–Ga1–Cl1 97.04(4); N1–Ga1–Cl2 97.39(4); Cl1–Ga1–Cl2 103.82(2); Ga1–Fe1–C1 85.32(5); Ga1–Fe1–C2 92.06(5); C1–Fe1–C2 92.38(7).

The financial support of this work by the *Deutsche Forschungsgemeinschaft* (Fi-502/2-1, 2-2; habilitation stipend for R. A. F.) and by the *"Friedrich-Schiedel Foundation"* is gratefully acknowledged. The authors also wish to thank Prof. *W. A. Herrmann* for generous support.

Experimental

All manipulations were undertaken by use of standard Schlenk, high-vacuum line and glove-box techniques under inert gas (purified argon). However, a modified special reaction vessel[37] was very advantageous to minimize undesired hydrolysis of the extremely air-sensitive compounds: The two arms (l = 25 cm, ∅ = 45 mm)

Table 8. Characteristic mass-spectrometric data of selected complexes

Compound	*No.*	*Type*	*characteristic fragments: m/z (rel. int %) [assignment]*
$Cp(CO)_3Cr\text{-}GaCl_2(NMe_3)$	**1a**	CI	342 (15) [M^+ - NMe_3]; 152 (100) [$CpCrCl^+$]
$Cp(CO)_3Mo\text{-}GaCl_2(NMe_3)$	**2a**	CI	330 (2) [M^+ - 2CO - NMe_3]; 200 (100) [$Cl_2GaNMe_3^+$]
$Cp(CO)_3W\text{-}GaCl_2(NMe_3)$	**3a**	CI	342 (15) [M^+ - Cl - NMe_3]; 58 (100) [$H_2CNMe_2^+$]
$Cp(CO)_3Cr\text{-}Ga[(CH_2)_3NMe_2](Cl)$	**1b**	CI	393 (12) [M^+]; 58 (100) [$H_2CNMe_2^+$]
$Cp(CO)_3W\text{-}Ga[(CH_2)_3NMe_2](Cl)$	**3b**	CI	525 (1) [M^+]; 190 (100) [$ClGa\{(CH_2)_3NMe_2\}^+$]
$(CO)_5Mn\text{-}GaEt_2(C_7H_{13}N)$	**4d**	CI	462 (70) [$(M + C_4H_8)^+$ - Et]; 112 (100) [$C_7H_{13}NH^+$]
$Cp(CO)_2Fe\text{-}GaCl_2(NMe_3)$	**5a**	CI	290 (4) [M^+ - 2CO - NMe_3]; 58 (100) [$H_2CNMe_2^+$]
$(CO)_4Co\text{-}GaCl_2(NMe_3)$	**6a**	CI	343 (1) [M+ - CO]; 200 (100) [$Cl_2GaNMe_3^+$]
$(CO)_4Co\text{-}GaEt_2(NMe_3)$	**6c**	EI*	357 (5) [M+]; 128 (30) [CoGa+]; 127 (100) [$GaEt_2^+$]
$(CO)_4Co\text{-}Ga[(CH_2)_3NMe_2](Cl)$	**6j**	CI	333 (100) [M^+ - CO]; 247 (3) [M^+ - $\{(CH_2)_3NMe_2\}$]
$(PMe_3)(CO)_3Co\text{-}Ga[(CH_2)_3NMe_2](Cl)$	**6k**	EI	381 (8) [M^+ - CO]; 353 (13) [M^+ - 2CO]; 325 (10) [M^+ - 3CO]
$(PMe_3)(CO)_3Co\text{-}Ga[(CH_2)_3NEt_2](^tBu)$	**6m**	EI	402 (10) [M^+ - ^tBu]; 240 (100) [$\{(^tBu)Ga\{(CH_2)_3NEt_2\}^+$]
$(PPh_3)(CO)_3Co\text{-}Ga[(CH_2)_3NMe_2](Cl)$	**6n**	EI	568 (3) [$(M+H)^+$ - CO]; 561 (2) [$(M+H)^+$ - Cl]
$(PCy_3)(CO)_3Co\text{-}Ga[(CH_2)_3NEt_2](Me)$	**6q**	EI	621 (1) [M^+]; 280 (8) [PCy_3^+]; 198 (100) [$(Me)Ga\{(CH_2)_3NEt_2\}^+$]
$Cp(CO)Ni\text{-}Ga[(CH_2)_3NEt_2](Me)$	**7d**	CI	304 (4) [M^+ - CO - Me]; 198 (100) [$(Me)Ga\{(CH_2)_3NEt_2\}^+$]

CI: Chemical ionization with isobutane (C_4H_{10}). – EI: Electron impact ionization, 70 eV. – [*] EI, 50 eV.

Table 9. Crystallographic and data collection parameters

	6a	**6t**	**5a**
formula	$C_{28}H_{31}ClCoGaNO_3P$	$C_{29}H_{34}CoGaNO_3P$	$C_{10}H_{14}Cl_2FeGaNO_2$
fw	624.6	604.2	376.7
space group	$P\bar{1}$ (No. 2)	$P2_1/c$ (No. 14)	$P2_1/n$ (No. 14)
T, °C	-20±1	+25±1	-80±1
a, pm	927.1(2)	987.6(2)	918.1(1)
b, pm	1147.0(3)	1239.0(2)	1214.3(1)
c, pm	1416.1(4)	2442(1)	1282.0(1)
α, deg	85.12(2)		
β, deg	85.23(2)	94.10(3)	106.27(1)
γ, deg	75.21(2)		
V, 10^6 pm^3	1447	2981	1372
Z	2	4	4
ρ_{calc} g cm^{-3}	1.433	1.34	1.824
μ (MoKα), cm^{-1}	16.7	15.4	34.0
transm. range, %	83.59 - 99.99	92.8-99.9	84.94-99.87
no. of reflns	5424	5618	2686
no. of obs. reflns	4650	4062	2266
no. of reflns used	4114	3300	2207
with	I > 2.0*σ(I)	I >1.5*σ(I)	I >1.0*σ(I)
R[a]	0.066	0.063	0.019
R_w[b]	0.059	0.056	0.020

[a] $R = \Sigma(\| F_o \| - \| F_c \|)/\Sigma \| F_o \|$. – [b] $R_w = [\Sigma_w(\| F_o \| - \| F_c \|)^2/\Sigma_w F_o^2]^{1/2}$.

Figure 5. AUGER-electron survey spectrum of a typical thin CoGa film grown from precursor $(CO)_4Co-GaEt_2(NMe_3)$ (**6c**) using a horizontal hot wall tube reactor at 350°C and 1 Pa in the absence of carrier gases; the level of impurities (C, N, O) is close to the detection limit of the method (0.5–1 atom-%)

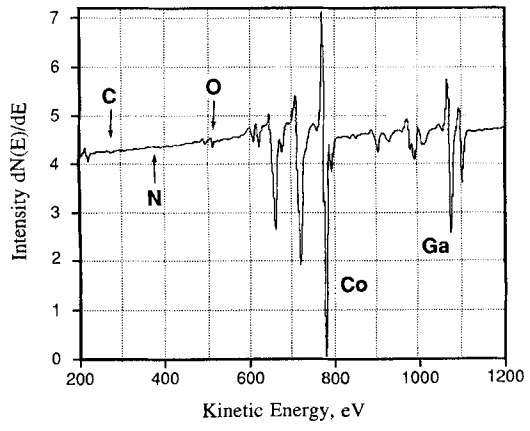

of the vessel are attached to each other at an angle of 120° and separated by a D3 glass frit. The first part is equipped with two ground glass joints, to which two side arm dumpers are attached. A 50-ml round bottom flask is mounted to the the second part of the vessel in the same manner. The whole reaction vessel is pivoted (270°) connected to a greaseless high-vacuum line (base pressure < 10^{-4} Torr)[38]. Solvents were dried under argon according to standard methods; *n*-pentane and toluene were stored over Na/K alloy, diethyl ether and THF over potassium benzophenoate (residual water <1 ppm, Karl-Fischer). – Infrared spectra were recorded as thin films (dry nujol mull) or solutions between carefully dried CaF_2 plates with a Perkin Elmer 1600 FT-IR instrument (sample preparation in the glove box). – JEOL JNM-GX400 and JNM-GX270 spectrometer were used for NMR spectroscopy. ^{1}H- and ^{13}C-NMR spectra were referenced to internal solvent and corrected to TMS. ^{31}P-NMR spectra: 80% aqueous H_3PO_4 (external standard). All samples for NMR spectra were placed in high-vacuum sealed NMR tubes, using carefully dried deuterated solvents. – Mass spectra were recorded with a Varian MAT 311-A instrument (EI spectra) and with a Varian MAT FS-90 instrument (CI and FI spectra). – Melting points were determined in sealed capillaries

and are not corrected. Abbreviations are as follows: Me = CH_3, Et = C_2H_5, Ph = C_6H_5, *i*Bu = isobutyl, *t*Bu = *tert*-butyl, Np = neopentyl. – Elemental analysis were provided by the Microanalytic Laboratory of the Technical University at Munich. – The numbering Scheme of the compounds is given in Table 2. The starting gallium compounds were synthesized according to literature procedures. The analytical and spectroscopic data of the new compounds are compiled in Tables 2–9.

1) General Procedures for the Synthesis of the Organogallio Transition Metal Carbonylate Complexes $(CO)_nM-GaR_2(Do)$ (**8a–e**, **10a–c**; M = Mn, Co; R = H, alkyl, halide; Do = THF, NMe_3, quinuclidine): The syntheses were conducted in the special reaction vessel described above, which was connected to a high-vacuum line with a base pressure ≤ 0.1 Pa (10^{-4} Torr). To a suspension of the solvent free, finely ground transition metal carbonylate $K[M(CO)_n]$ (typically 1–5 mmol) in 50 ml of *n*-pentane an equimolar amount of the respective alkylgallium halide was slowly added at −78 °C. After warming up to room temp. and stirring for 1 h the mixture was filtrated and the white residue obtained was extracted several times with *n*-pentane by recondensing the solvent into the first arm of the reaction vessel. The combined extracts were concentrated. Upon slow cooling to −30 °C the complexes separated as almost colorless, analytically pure well-shaped large crystals. Typical yields range between 80 and 95% of the theory. The compounds sublime around 40–80 °C (ca. 1 Pa dyn. vacuum).

2) General Procedure for the Synthesis of the Transition Metal Gallium Complexes of the Formulas $L(CO)_nM-GaCl_2(Do)$ (**5a**, **6a**, **7a**, **8a**, **10k**, **11a**: M = Cr, Mo, W, Fe, Co, Ni; L = CO, PMe_3, η^5-C_5H_5; Do = NMe_3, quinuclidin, THF) *and* $L(CO)_nM-Ga[(CH_2)_3NMe_2]Cl$ (**5b**, **6b**, **7b**, **9d**, **11c**; M = Cr, Mo, W, Fe, Ni; L = CO, PMe_3, η^5-C_5H_5): To a solution of $K[L(CO)_nM]$ in 50 ml of THF (typically 5 mmol; c = 1 mol/l) an equimolar amount of the respective gallium halide $Cl_3Ga(Do)$ or $Cl_{2-a}R_aGa[(CH_2)_3NMe_2]$ was slowly added at −78 °C. The reaction mixture was allowed to warm up to room temp. within 1 h. After stirring for 2 h the reaction mixture was filtered and the solvent removed in vacuo. The obtained residue was extracted several times with portions of 25–50 ml of methylene chloride or toluene. The combined and filtrated extracts were then concentrated and the products crystallized upon slow cooling to −30 °C within several days. Typical yields range between 85 and 95%.

3) trans-Tricarbonyl{chloro-[3-(dimethylamino)propyl]gallio}-(trimethylphosphane)cobalt (**6k**) *and trans-{tert-Butyl-[3-(diethylamino)propyl]gallio}tricarbonyl(trimethylphosphane)cobalt* (**6m**): 0.33 g (1.27 mmol) of $[(Me_3P)(CO)_3Co]K$ was treated with 0.287 g (1.266 mmol) of $Cl_2Ga[(CH_2)_3NMe_2]$ as described above. Crystallization from diethyl ether/*n*-pentane mixtures yielded 0.33 g (63.5%) of **6k**. Compound **6m** was synthesized similarly. – **6m**: ^{31}P NMR (161.9 MHz, [D$_8$]toluene, −85 °C): δ = 12.8 (s, CoP).

4) trans-Tricarbonyl{[3-(diethylamino)propyl]methylgallio}(tricyclohexylphosphane)cobalt (**6q**) *and related derivatives* **6n**, **6r–t**: 370 mg (1.0 mmol) of $(CO)_4Co-Ga[(CH_2)_3NEt_2](Me)$ and 300 mg (1.1 mmol) of tricyclohexylphosphane were dissolved in 5 ml of toluene. The reaction vessel (e.g. a Schlenk tube of the dimensions 15 by 2.5 cm) was sealed in vacuo after freezing of the solution to −196 °C. The mixture was subsequently heated to 80 °C for 1 h. After cooling to room temp. all volatile components were removed in vacuo. The obtained orange-yellow oily residue was washed twice with 2.5 ml of *n*-pentane at 0 °C. The product was crystallized from 5 ml of a toluene/*n*-pentane mixture at −30 °C during several days. Yield: 520 mg (85%) of **6q** as small, pale yellow analytically pure crystals. The compounds **6n** and **6r–t** were synthesized analogously. – **6n**: ^{31}P NMR (161.9 MHz, [D$_8$]toluene, 80 °C): δ = 61.7. – **6q**: ^{31}P NMR (161.9 MHz, [D$_8$]toluene, 25 °C): δ = 70.1.

5) trans-{tert-Butyl-[3-(dimethylamino)propyl]gallio}tricarbonyl(triphenylphosphane)cobalt (**6p**). – *General Procedure for the Alkylation of Residual Chloride Functions in Compounds of the Type* $L(CO)_nM-GaClR(Do)$: 850 mg (1.43 mmol) of **6n** was dissolved in 50 ml of toluene and the solution was subsequently treated with a solution of *tert*-butyllithium (90 mg, 1.43 mmol) in 20 ml of toluene at −78 °C. The stirred mixture was allowed to warm up to room temp. within 12 h. After filtration and removal of the solvent from the filtrate by vacuum distillation at room temp. the residue was dissolved into 10 ml of diethyl ether. To this solution a small amount of *n*-pentane was added until the mixture became cloudy. Crystallization at −30 °C yielded 640 mg (72%) of **6p**. – ^{31}P NMR (161.9 MHz, [D$_8$]toluene, 25 °C): δ = 62.2.

Single-Crystal Structure Analysis of **5a** *and* **6s–t**: Suitable crystals of **5a** and **6s–t** were selected and transferred to Lindemann capillaries, which were subsequently sealed under argon and mounted to an automatic four-circle diffractometer (CAD4 Enraf-Nonius; graphite monochromated Mo-$K_{\bar{\alpha}}$ radiation: λ = 0.71073 Å). The crystallographic and data collection parameters are summarized in Table 9. The lattice parameters were refined on the basis of 25 reflections at high diffraction angles. The cell parameters were checked with the cell reduction programs "TRACER" and "LEPAGE". The intensities were collected by the ω-scan mode. The intensity of the reflections and the orientation of the crystal during the measurement were routinely checked. In the case of **6t** intensity correction due to some intensity variations of the control reflections was performed. After LP correction (**6s–t**, **5a**), empirical absorption correction on the basis of Ψ-scan data with the program "EAC" (**6s**, **5a**) and averaging of the remaining reflections were used for the structure solution and refinement. The structure solution was performed with Patterson methods[39] and subsequent difference Fourier techniques[40]. For **6s** the structure was solved by using direct methods[39]. Atomic form factors for neutral atoms[41] and anomal dispersion were considered[42]. All 14 hydrogen atom positions of **5a** were obtained from difference Fourier syntheses and were refined freely. For **6s–t** the hydrogen atom positions were placed in ideal geometry with collective isotropic thermal parameters and included into the structure factor calculations, but not refined. The five-membered heterocyclic chelate ring of **6s–t** is disordered. For **6s** the disorder was not resolved. For **6t** the disorder was resolved as discussed in the main text. Further details of the crystal structure investigations are available from the Fachinformationszentrum Karlsruhe, Gesellschaft für wissenschaftlich-technische Information mbH, D-76344 Eggenstein-Leopoldshafen (Germany), on quoting the depository numbers CSD-56977 (**6s**) and CSD-59007 (**5a**, **6t**), the names of the authors and the journal citation.

☆ Dedicated to Prof. *Hubert Schmidbaur* on the occasion of his 60th birthday.

[1] [1a] R. A. Fischer, J. Behm, *Chem. Ber.* **1992**, *125*, 37–42. – [1b] R. A. Fischer, J. Behm, T. Priermeier, *J. Organomet. Chem.* **1992**, *429*, 275–286. – [1c] R. A. Fischer, J. Behm, T. Priermeier, W. Scherer, *Angew. Chem.* **1993**, *105*, 776–778; *Angew. Chem. Int. Ed. Engl.* **1993**, *32*, 772–774. – [1d] R. A. Fischer in *Chemical Perspectives of Microelectronic Materials III* (Eds.: C. R. Abernathy, J. C. W. Bates, D. A. Bohling, W. S. Hobson), Materials Research Society, Pittsburgh, PA, **1993**, 267–273. – [1e] R. A. Fischer, W. Scherer, M. Kleine, *Angew. Chem.* **1993**, *105*, 778–780; *Angew. Chem. Int. Ed. Engl.* **1993**, *32*, 774–776. – [1f] R. A. Fischer, T. Priermeier, W. Scherer, *J. Organomet. Chem.* **1993**, *459*, 65–71. – [1g] R. A. Fischer, M. M. Schulte, T. Priermeier, *J. Organomet. Chem.* **1995**, in press. – [1h] R. A.

Fischer, A. Miehr, M. Schulte, *Adv. Mater.* **1995**, *7*, 58–61. – [1i] R. A. Fischer, A. Miehr, M. M. Schulte, E. Herdtweck, *J. Chem. Soc. Chem. Commun.* **1995**, 337–338.
[2] [2a] M. Herberhold, G.-X. Jin, *Angew. Chem.* **1994**, *106*, 1016–1018; *Angew. Chem. Int. Ed. Engl.* **1994**, *33*, 964–966. – [2b] A. Grohmann, *Nachr. Chem. Tech. Lab.* **1995**, *43*, 124–131, p. 130.
[3] [3a] I. P. Beletskaya, A. Z. Voskoboynikov, E. B. Chuklanova, N. I. Kirillova, A. K. Shestakova, I. N. Parshina, A. I. Gusev, G. K.-I. Magomedov, *J. Am. Chem. Soc.* **1993**, *115*, 3156–3166. – [3b] R. S. Sternal, C. P. Brock, T. J. Marks, *J. Am. Chem. Soc.* **1985**, *107*, 8270–8272. – [3c] R. S. Sternal, T. J. Marks, *Organometallics* **1987**, *6*, 2621–2623.
[4] R. A. Fischer, J. Behm, *J. Organomet. Chem.* **1991**, *413*, C10–C14.
[5] J. N. StDenis, W. Butler, M. D. Glick, J. P. Oliver, *J. Organomet. Chem.* **1977**, *129*, 1–16.
[6] A. J. Conway, P. B. Hitchcock, J. D. Smith, *J. Chem. Soc., Dalton Trans.* **1975**, 1945–1949.
[7] U. Flörke, P. Balsaa, H.-J. Haupt, *Acta Crystallogr., Sect. C* **1986**, *C42*, 275–277.
[8] H.-J. Haupt, P. Balsaa, U. Flörke, *Z. Anorg. Allg. Chem.* **1988**, *557*, 69–81.
[9] H. Preut, H. J. Haupt, *Chem. Ber.* **1974**, *107*, 2860–2869.
[10] H.-J. Haupt, U. Flörke, H. Preut, *Acta Crystallogr., Sect. C* **1986**, *C42*, 665–667.
[11] A. H. Cowley, A. Decken, C. A. Olazábal, N. C. Norman, *Inorg. Chem.* **1994**, *33*, 3435–3437.
[12] X. He, R. A. Bartlett, P. P. Power, *Organometallics* **1994**, *13*, 548–552.
[13] R. M. Campbell, L. M. Clarkson, W. Clegg, D. C. R. Hockless, N. L. Pickett, N. C. Norman, *Chem. Ber.* **1992**, *125*, 55–59.
[14] M. Schollenberger, B. Nuber, M. L. Ziegler, E. Hey-Hawkins, *J. Organomet. Chem.* **1993**, *460*, 55–66.
[15] M. L. H. Green, P. Mountford, G. J. Smout, S. R. Speel, *Polyhedron* **1990**, *9*, 2763–2765.
[16] J. C. Vanderhooft, R. D. Ernst, F. W. C. Junior, R. J. Neustadt, T. H. Cymbaluk, *Inorg. Chem.* **1982**, *21*, 1876–1880.
[17] R. A. Fischer, H. D. Kaesz, S. I. Khan, H.-J. Müller, *Inorg. Chem.* **1990**, *29*, 1601–1602.
[18] R. A. Fischer, J. Behm, E. Herdtweck, C. Kronseder, *J. Organomet. Chem.* **1992**, *437*, C29–C34.
[19] C. A. Olazábal, A. H. Cowley, *Organometallics* **1994**, *13*, 421–423.
[20] M. Y. Darensbourg, *Prog. Inorg. Chem.* **1985**, *33*, 221–274.
[21] J. R. Clipperfield, S. Clark, D. E. Webster, H. Yusof, *J. Organomet. Chem.* **1991**, *421*, 205–313.
[22] B. Gerz, E. Hahn, W.-W. d. Mont, J. Pickardt, *Angew. Chem.* **1984**, *96*, 69–70; *Angew. Chem. Int. Ed. Engl.* **1984**, *23*, 61–62.
[23] R. G. Pearson, *J. Am. Chem. Soc.* **1980**, *102*, 1541–1547.
[24] J. M. Burlitch, M. E. Leonowicz, R. B. Petersen, R. E. Hughes, *Inorg. Chem.* **1978**, *18*, 1097–1105.
[25] M. Nitay, M. Rosenblum, *J. Organomet. Chem.* **1977**, *136*, C23–C25.
[26] J. F. Hartwig, S. Huber, *J. Am. Chem. Soc.* **1993**, *115*, 4908–4909.
[27] H. Memmler, S. Friedrich, L. H. Gade, W.-S. Li, M. McPartlin, *Angew. Chem.* **1994**, *106*, 705–708; *Angew. Chem. Int. Ed. Engl.* **1994**, *33*, 675–678.
[28] [28a] J. Sundermeyer, D. Runge, *Angew. Chem.* **1994**, *106*, 1328–1331; *Angew. Chem. Int. Ed. Engl.* **1994**, *33*, 1255–1257. – [28b] J. Sundermeyer, D. Runge, J. S. Field, *Angew. Chem.* **1994**, *106*, 679–682; *Angew. Chem. Int. Ed. Engl.* **1994**, *33*, 678–681.
[29] C. Kronseder, T. Schindler, C. Berg, R. A. Fischer, G. Niedner-schatteburg, V. Bondybey, *J. Organomet. Chem.* **1994**, *475*, 247–256.
[30] A. Bondi, *J. Phys. Chem.* **1964**, *68*, 441–451.
[31] T. A. Albright, J. K. Burdett, M. H. Whangbo in *Orbital Interactions in Chemistry*, Wiley, New York, **1985**.
[32] L. M. Golubinskaya, A. V. Golubinskii, V. S. Mastryukov, L. V. Vilkov, V. I. Bregadze, *J. Organomet. Chem.* **1976**, *117*, C4–C6.
[33] H. Schumann, U. Hartmann, W. Wassermann, O. Just, A. Dietrich, L. Pohl, M. Hostalek, M. Lokai, *Chem. Ber.* **1991**, *124*, 1113–1119.
[34] R. A. Fischer, E. Herdtweck, T. Priermeier, *Inorg. Chem.* **1994**, *33*, 934–943.
[35] J. C. Carter, G. Jugie, R. Eujalbert, J. Galz, *Inorg. Chem.* **1978**, *17*, 1248–1254.
[36] [36a] A. G. Orpen, N. G. Connelly, *J. Chem. Soc. Chem. Commun.* **1985**, 1310–1311. – [36b] D. S. Marynick, *J. Am. Chem. Soc.* **1984**, *106*, 4064–4065. – [36c] S.-X. Xiao, W. C. Trogler, D. E. Ellis, Z. Berkovitch-Yellin, *J. Am. Chem. Soc.* **1983**, *105*, 7033–7037. – [36d] G. Pacchioni, P. S. Bagus, *Inorg. Chem.* **1992**, *31*, 4391–4398.
[37] W. Strohmeier, *Chem. Ber.* **1955**, *88*, 1218–1223.
[38] A. L. Wada, J. L. Dye, *J. Chem. Educ.* **1985**, *62*, 356–358.
[39] G. M. Sheldrick, SHELXS-86, *Program for Crystal Structure Determination*, Universität Göttingen, **1986**.
[40] B. A. Frenz, *The ENRAF-NONIUS CAD4 SDP SYSTEM*, Computing in Crystallography, DELFT University Press, Delft/Holland **1978**.
[41] D. T. Cromer, J. T. Waber, *International Tables of Crystallography*, Vol. IV, Tab. 2.2.B (Atomformfaktoren), Kynoch Press, Birmingham/England, **1974**.
[42] D. T. Cromer, *International Tables of Crystallography*, Vol. IV, Tab. 2.3.1 (Anomale Dispersion), Kynoch Press, Birmingham/England, **1974**.
[43] A. L. Spek, The "EUCLID" package, in *Computational Crystallography* (Ed. D. Sayre), Clarendon Press, Oxford **1982**, p. 528.
[44] E. Keller, SCHAKAL, *Program for the Graphical Representation of Molecular Modells*, Kristallographisches Institut, Universität Freiburg, Germany, **1986/1988**.

[95035]